

## §15. Energy Level Structure of $\text{Er}^{3+}$ Free Ion and $\text{Er}^{3+}$ Ion in $\text{Er}_2\text{O}_3$ crystal

Gaigalas, G., Rynkun, P., Radžiūtė, L. (Vilnius Univ.), Jönsson, P. (Malmö Univ.), Kato, D.

**i) Introduction** The basic, and novel, idea of this work is to calculate the energy spectrum and the transition parameters for the free ion  $\text{Er}^{3+}$  in an *ab initio* approach and then apply the point charge crystal field as a perturbation to obtain the  $\text{Er}_2\text{O}_3$  Stark components of the  $[\text{Xe}]4f^{11}4I_{15/2}^o$  level. The calculations were performed using the GRASP2K<sup>1)</sup> which is based on the multiconfiguration Dirac-Hartree-Fock method and relativistic configuration interaction.

**ii) Calculation and results of  $\text{Er}^{3+}$  free ion** The change of the positions of levels  $4S_{3/2}$  and  $4F_{9/2}$  when increasing the active sets and opening deeper closed shells is demonstrated in Fig. 1. It is seen that calculations with the active set  $n = 6$  including single and double substitutions from the valence, core and core-valence shells, when only  $4d$  and  $4p$  excitations are taken from the core (the case SD  $V+CC+CV$   $4d$   $4p$ ), lead to energy level positions close to the experimental ones. Further increase of the active set or opening of deeper core shells do not significantly change the results (see Fig. 1).

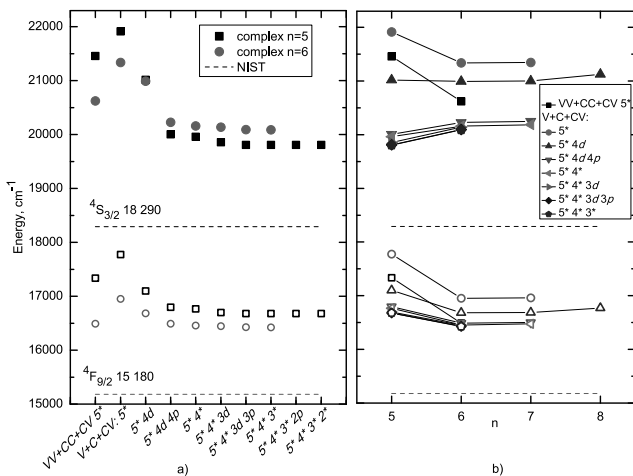


Fig. 1: Convergence of the energy for  $4f^{11}4S_{3/2}$  (filled symbols) and  $4F_{9/2}$  (empty symbols) levels of  $\text{Er}^{3+}$ : a) opening core shells and b) increasing principal quantum number of the active set in different strategies. In one case, notated  $VV + CC + CV$ , SD excitation were made without restrictions.

**iii) Method of accounting for the crystal field effects** In order to calculate the splitting of the ionic energy levels  $\gamma J$  in solids, the crystal field effects must

be included. Instead of using the simplified treatment of the crystal field effects based on the Stevens' operator-equivalent method we used the fully *ab-initio* method. In order to be able to perform crystal-field calculations the GRASP2K<sup>1)</sup> relativistic atomic structure programs been extended. This extension include programs for the crystal field operator matrix element calculation and diagonalization of matrix of full atomic Hamiltonian (including matrix elements between different atomic state functions).

**iv) Calculations of the crystal-field splitting of  $\text{Er}^{3+}$  ion in the  $\text{Er}_2\text{O}_3$  compound** Table I compares the results obtained in this study with the results of other authors using semi-empirical methods as well as with the experimental results. Experimental data of Stark components were obtained for single crystals  $\text{Er}_2\text{O}_3$  and  $\text{Er}^{3+}:\text{Y}_2\text{O}_3$ <sup>2)</sup>. Semi-empirical Stark levels were calculated using a Hamiltonian containing atomic and crystal field terms. In other experiments  $\text{Er}_2\text{O}_3$  powder was used<sup>3)</sup>. Experiment have shown, that powder have also cubic symmetry. Data from experiment were used in semi-empirical methods to compute crystal field parameters and Stark levels. In another experiment the Stark components of lowest three levels were measured by absorption spectroscopy in  $\text{Er}_2\text{O}_3$  and  $\text{ErF}_3$ <sup>4)</sup>. As can be seen from the comparative analysis of the results, the *ab-initio* point charge crystal field approximation for  $\text{Er}^{3+}$  in  $\text{Er}_2\text{O}_3$  leads to a bigger splitting compared with the experimental one. In order to get more accurate theoretical results, the further development of the theory is needed.

Table I: Comparison of computed energy (Stark) levels (in  $\text{cm}^{-1}$ ) of  $\text{Er}^{3+}$  ( $4f^{11}4I_{15/2}^o$ ) in  $\text{Er}_2\text{O}_3$  crystal field with other theories and experiment.

Experiment		Semi-empirical			Theoretical	
2)	3)	4)	2)	3)	4)	This work
0	0	0	1	2	0	0.00
38	36	39.5	36	37	11.6	495.38
75	69	75.3	66	65	79.4	797.41
88	86	89.0	93	81	107.7	995.97
159	162	260.1	169	157	154.8	1287.26
265	263	349.6	262	265	176.7	1709.93
490	484	488.6	477	483	194.3	2213.95
505	503	531.2	502	506	249.8	2609.69

- 1) P. Jönsson *et al.*, Comput. Phys. Commun. (2013) vol.184 2197.
- 2) J.B. Gruber *et al.*, J. Appl. Phys. (2010) vol.108 023109.
- 3) M. Dammak and De-Long Zhang, Journal of Alloys and Compounds (2006) vol.407 8.
- 4) N. Magnani *et al.*, Phys. Status Solidi C (2007) vol.4 1209.